

4.5 Autolysin Profiles of Laboratory-Derived VISA and Parental Strains

To examine a correlation of whole cell autolysis and autolytic enzymes, extracted autolysins were characterized. The zymographic analyses of extracted autolysins of the laboratory-derived hVISA strains with vancomycin MICs of 4 µg/ml and VISA with the MICs of 7 µg/ml and their parental strains are presented in Figures 4.10 to 4.15. Parental strains KY, SS, UH7, UH9, Mu3, and UH35 expressed three major autolytic bands of bigger than 118 kDa, about 118 kDa, and 49 kDa that may corresponding to the unprocessed autolysin (bifunctional product of the *atl* gene; 138 kDa), the intermediately processed autolysin (115 kDa), and the endo- β -*N*-acetylglucosaminidase (GL) (51 kDa), respectively (Fig. 4.10 to 4.15) (Hanaki *et al.*, 1998; Antignac *et al.*, 2007). Weaker bands that may corresponding to the autolysin processing intermediates at approximately bigger than 90 kDa and *N*-acetylmuramyl-L-alanine amidase at 62 kDa were also observed.

The hVISA strains with vancomycin MICs of 4 µg/ml expressed three major autolytic bands and two weaker bands corresponding to those of their parental strains. KY-8, SS-8, and UH9-8 had no differences of intensities of autolytic bands comparing to those of their parental strains (Fig. 4.10 and 4.11). UH7-8 expressed slight increased intensities of autolytic bands comparing to its parental strain (Fig. 4.11). Contrary, intensities of autolytic bands of Mu3-8 and UH35-8 were less than those of their parental Mu3 and UH35, respectively (Fig. 4.12).

VISA derivatives with vancomycin MICs of 7 µg/ml, KY-8-1, SS-8-1, UH7-8-1, UH9-8-1, and Mu3-8-1 showed reduced intensities of autolytic bands comparing to those of their parental strains (Fig. 4.13 to 4.15). This may due to reduced amounts or activities of autolytic enzymes (Koehl *et al.*, 2004; Utaida *et al.*, 2006). These are consistent with whole cell autolysis profiles of parental strains and their derivatives in that VISA had reduced autolytic activities comparing to those of parental strains (Fig. 4.2B to 4.5B). However, there had no differences of autolytic band intensities between VISA UH35-8 and UH35 (Fig. 4.15).

4.6 Effects of Vancomycin on Autolysin Profiles

When vancomycin was presented in the media, all VSSA strains had no differences of intensities of autolytic bands (Fig. 4.10 to 4.15). However, parental strain KY in the group of VISA with MICs of 7 µg/ml expressed slight increased intensities of autolytic bands when

vancomycin was presented in the medium (Fig. 4.13). Contrary, UH35 had decreased intensities of the bands (Fig. 4.15).

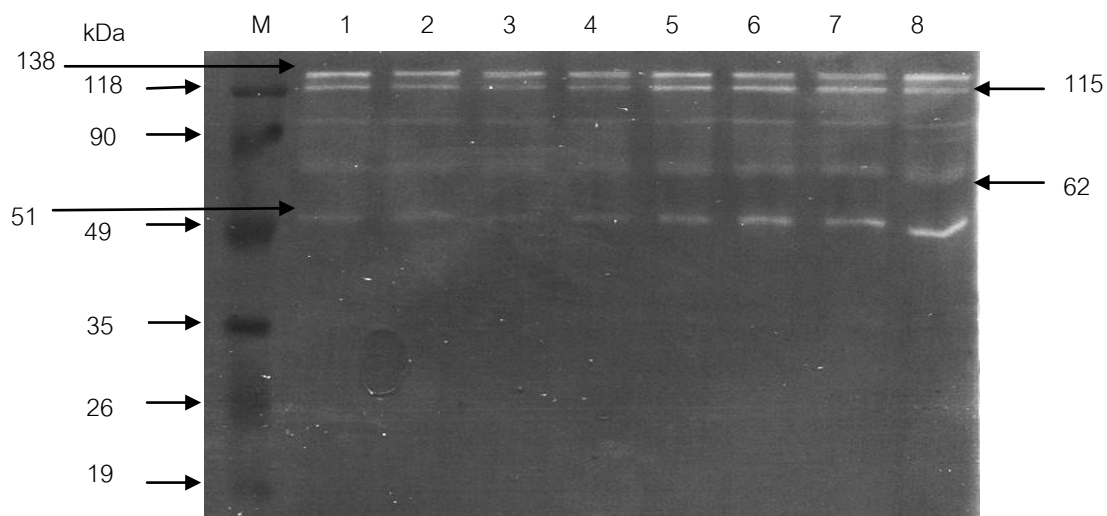
In the group of hVISA (vancomycin MICs of 4 µg/ml), KY-8 and UH7-8 showed no different intensities of autolytic bands (Fig. 4.10 and 4.11). SS-8 and Mu3-8 showed slight increased intensities of autolytic bands when vancomycin was presented (Fig. 4.10 and 4.12). UH9-8 and UH35-8 had slight reduced intensities autolytic bands (Fig. 4.11 and 4.12). These results were inconsistent with whole cell autolysis in that KY-8 and UH35-8 had increased whole cell autolysis when vancomycin was presented in the buffer. Other hVISA strains had no significant differences (Fig. 4.2A to 4.6A).

When vancomycin MICs increased to 7 µg/ml, increased intensities of autolytic bands were observed for KY-8-1 when grown in presence of vancomycin (Fig. 4.13). VISA derivatives UH35-8 showed increased intensities of the autolytic bands with the presence of vancomycin (Fig. 4.15). SS-8-1, UH7-8-1, UH9-8-1, and Mu3-8-1, however, had no differences of the band intensities comparing to those of grown in the absence of the drug (Fig. 4.13 to 4.15). These results suggested that vancomycin affected differently to autolysin profiles of each strain. These may reflect the regulation of autolysin genes in each bacterial strain. Mongodin *et al.* (2003) reported that *atl* genes were upregulated in some VISA strains when they were passaged in vancomycin (Mongodin *et al.*, 2003). Kuroda *et al.* (2003), however, reported that *atl* gene were downregulated when bacteria exposed to vancomycin (Kuroda *et al.*, 2003).

However, the effects of vancomycin on autolysin profiles were inconsistent with whole cell autolysis profiles. Utaida *et al.* (2006) reported the differences of vancomycin effect on autolytic activities between whole cell autolysis and zymograms and implied that the regulation of autolytic activity was complex. The regulation can occur at different levels such as cell wall level (Neuhaus and Baddiley, 2003; Koehl *et al.*, 2004), autolytic activity system (Sieradzki and Tomasz, 2006), and at transcriptional level (Ingavale *et al.*, 2003; Kuroda *et al.*, 2003).

FIGURE 4.10

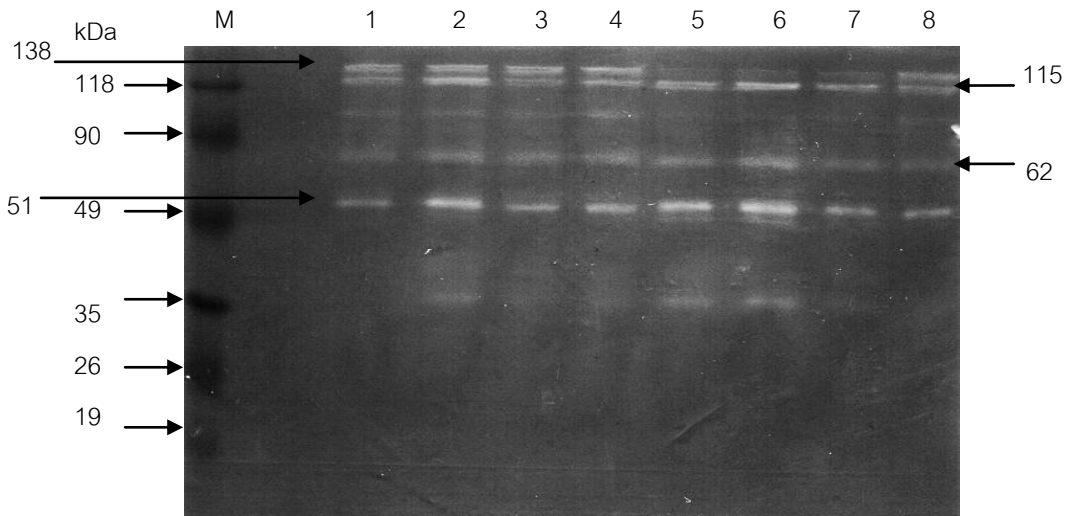
Autolysin Zymograms of KY, SS, and Their hVISA Derivatives



Parental strains KY and SS and hVISA derivatives KY-8 and SS-8 were grown in the absence and presence of vancomycin. Autolytic bands were observed as clear zones in the opaque gel containing *M. luteus* cells as substrate. Lanes: M, prestained molecular weight protein marker (Fermentas); 1 and 3, KY; 2 and 4, KY-8; 5 and 7, SS; 6 and 8, SS-8. Lanes 3, 4, 7, and 8 bacteria were grown in the presence of vancomycin at 0.5 $\mu\text{g}/\text{ml}$ for parental and 2 $\mu\text{g}/\text{ml}$ for hVISA strains.

FIGURE 4.11

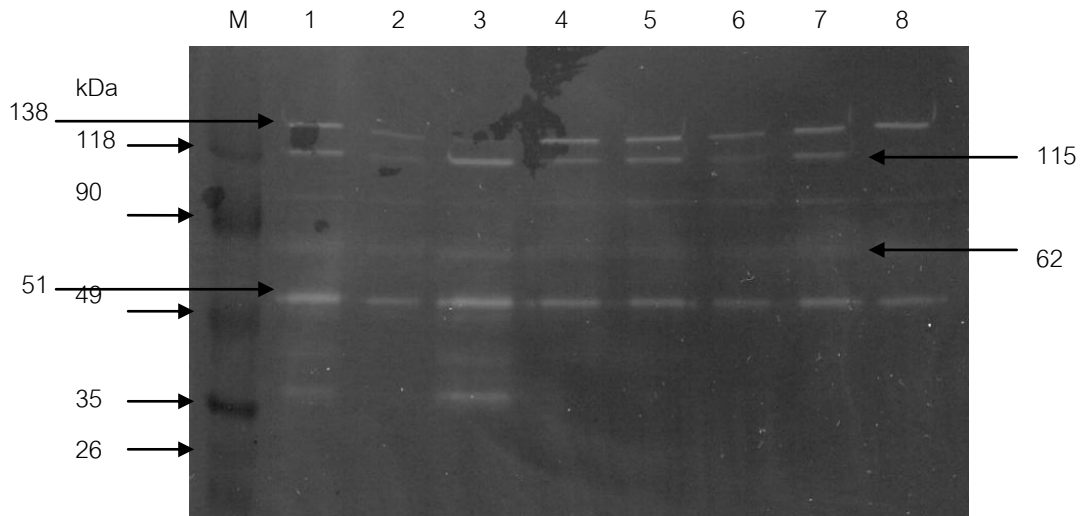
Autolysin Zymograms of UH7, UH9, and Their hVISA Derivatives



Parental strains UH7 and UH9 and hVISA derivatives UH7-8 and UH9-8 were grown in the absence and presence of vancomycin. Autolytic bands were observed as clear zones in the opaque gel containing *M. luteus* cells as substrate. Lanes: M, prestained molecular weight protein marker (Fermentas); 1 and 3, UH7; 2 and 4, UH7-8; 5 and 7, UH9; 6 and 8, UH9-8. Lanes 3, 4, 7, and 8 bacteria were grown in the presence of vancomycin at 0.5 $\mu\text{g/ml}$ for parental and 2 $\mu\text{g/ml}$ for hVISA strains.

FIGURE 4.12

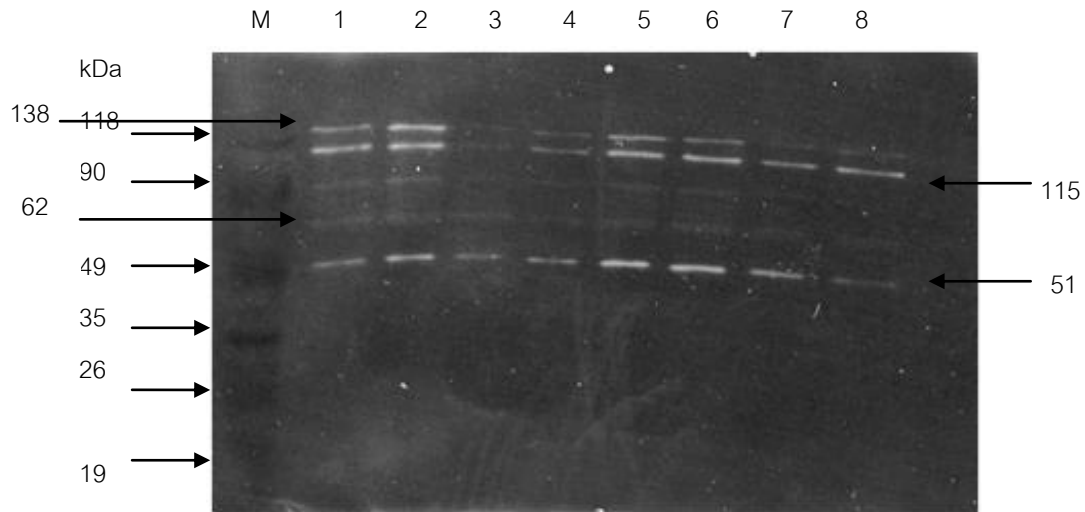
Autolysin Zymograms of Mu3, UH35, and Their hVISA Derivatives



Parental strains Mu3 and UH35 and hVISA derivatives Mu3-8 and UH35-8 were grown in the absence and presence of vancomycin. Autolytic bands were observed as clear zones in the opaque gel containing *M. luteus* cells as substrate. Lanes: M, prestained molecular weight protein marker (Fermentas); 1 and 3, Mu3; 2 and 4, Mu3-8; 5 and 7, UH35; 6 and 8, UH35-8. Lanes 3, 4, 7, 8 bacteria were grown in the presence of vancomycin at 0.5 $\mu\text{g/ml}$ for parental and 2 $\mu\text{g/ml}$ for hVISA strains.

FIGURE 4.13

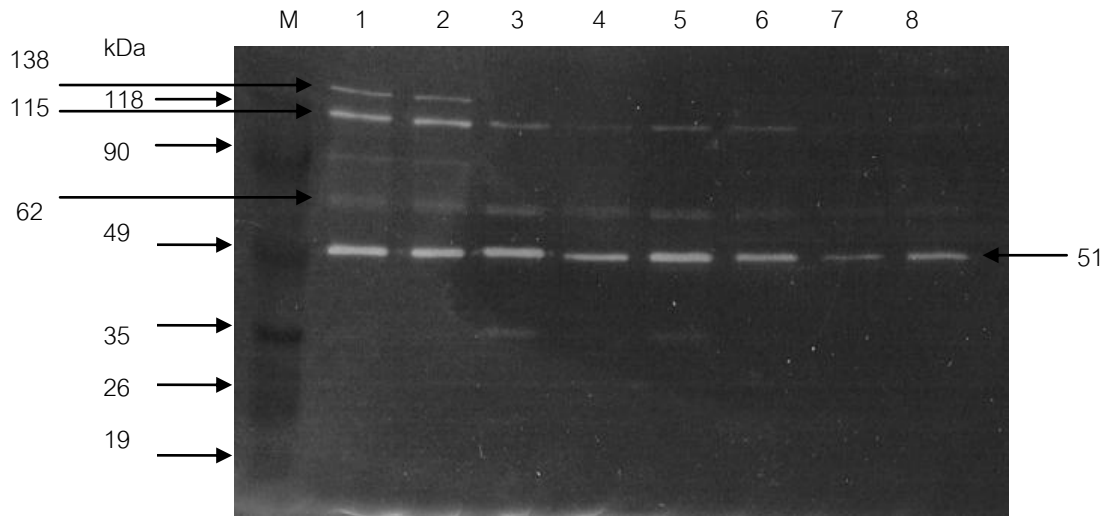
Autolysin Zymograms of KY, SS, and Their VISA Derivatives



Parental strains KY and SS and VISA derivatives KY-8-1 and SS-8-1 were grown in the absence and presence of vancomycin. Autolytic bands were observed as clear zones in gel containing *M. luteus* cells as substrate. Lanes: M, prestained molecular weight protein marker (Fermentas); 1-2, KY; 3-4, KY-8-1; 5-6, SS; 7-8, SS-8-1. Lanes 2, 4, 6, 8 bacteria were grown in the presence of vancomycin at 0.5 $\mu\text{g/ml}$ for parental and 3.5 $\mu\text{g/ml}$ for VISA strains.

FIGURE 4.14

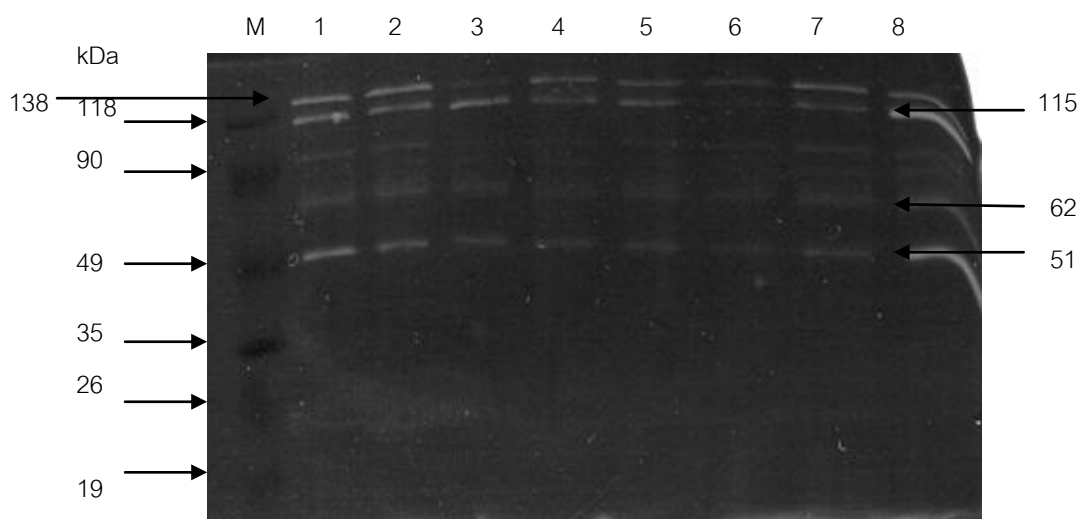
Autolysin Zymograms of UH7, UH9, and Their VISA Derivatives



Parental strains UH7 and UH9 and VISA derivatives UH7-8-1 and UH9-8-1 were grown in the absence and presence of vancomycin. Autolytic bands were observed as clear zones in gel containing *M. luteus* cells as substrate. Lanes: M, prestained molecular weight protein marker (Fermentas); 1-2, UH7; 3-4, UH7-8-1; 5-6, UH9; 7-8, UH9-8-1. Lanes 2, 4, 6, 8 bacteria were grown in the presence of vancomycin at 0.5 $\mu\text{g/ml}$ for parental and 3.5 $\mu\text{g/ml}$ for VISA strains.

FIGURE 4.15

Autolysin Zymograms of Mu3, UH35, and Their VISA Derivatives



Parental strains Mu3 and UH35 and VISA derivatives Mu3-8-1 and UH35-8-1 were grown in the absence and presence of vancomycin. Autolytic bands were observed as clear zones in gel containing *M. luteus* cells as substrate. Lanes: M, prestained molecular weight protein marker (Fermentas); 1-2, Mu3; 3-4, Mu3-8-1; 5-6, UH35; 7-8, UH35-8-1. Lanes 2, 4, 6, 8 bacteria were grown in the presence of vancomycin at 0.5 $\mu\text{g/ml}$ for parental and 3.5 $\mu\text{g/ml}$ for VISA strains.

4.7 Cell Wall Morphologies of VISA Derivatives and VSSA Strains

Altered cell wall morphologies are one of common features of VISA or VRSA strains (Pfeltz *et al.*, 2000; Cui *et al.*, 2003; Cui *et al.*, 2006). Cell wall morphologies of VISA derivatives with vancomycin MICs of 7 $\mu\text{g/ml}$ and their parental strains were determined by transmission electron microscopy as described in Material and Methods. Table 4.4 shows results of cell wall thickness measurement for VISA derivatives, KY-8-1, SS-8-1, UH7-8-1, UH9-8-1, and their VSSA strains. The statistical significant of data was evaluated at the significance level of 0.05. Almost VISA derivatives, KY-8-1, SS-8-1, and UH7-8-1, had significantly thicker cell walls than their parental strains (p -value = 0.001, 0.015, and 0.022, respectively). No significant difference of the wall thickness was observed for UH9-8-1 and its parental strain (p -value = 0.091). Transmission electron micrographs of VISA derivatives and their parental strains are shown in figures 4.16 to 4.19. Cell wall surfaces of KY-8-1, SS-8-1, and UH7-8-1 appeared to be more roughened than those of their parental strains (Fig. 4.16 to 4.18). The roughened cell wall was

not observed for UH9-8-1 (Fig 4.19). The results suggested that the thickened and roughened walls observed for VISA correlate with levels of vancomycin MICs of VISA derivatives. Cui *et al.* (2003) reported that *S. aureus* with reduced susceptibility to vancomycin had thickened cell wall and became thinner when bacteria decreased vancomycin MICs indicating that cell wall thickening correlated with vancomycin resistance and was common feature of VRSA or VISA (Cui *et al.*, 2003).

Previous reports revealed that the thickened cell wall and roughened surface were common features of VISA (Pfeltz *et al.*, 2000; Cui *et al.*, 2006). The studies of the resistance strains possessing thickened cell wall show that they have accumulation of cell wall materials including free D-alanyl-D-alanine and UDP-N-acetylmuramyl-pentapeptide in the surface of the cytoplasmic membrane which block the access of vancomycin to its target at the cytoplasmic membrane (Sieradzki *et al.*, 1997; Pfeltz *et al.*, 2000; Cui *et al.*, 2006). Therefore these features enable VISA or VRSA to prevent cell wall degradation from vancomycin (Cui *et al.*, 2006).

To observe effect of vancomycin on cell wall morphologies, vancomycin with concentrations of one-half of vancomycin MICs of each strain was included in the medium. The thickness cell wall and wall surfaces of all VISA derivatives including UH9-8-1 (p-value = 0.091) appeared to be not different between the absence and presence of vancomycin (Table 4.4 and Fig. 4.16 to 4.19). Pfeltz *et al.* (2000) reported that VISA had thickened and roughed cell wall when grown in the presence of vancomycin. However, the results are inconsistent with reports of VISA in this study. Almost parental strains had no differences in thickness and roughness when growing in the presence of vancomycin. Similarly, UH9 had no significant differences in thickness and roughness when growing in the presence of the drug (p-value = 0.460). However, UH7 had a slight thickened cell wall in the presence of vancomycin (p-value = 0.031) (Table 4.4). This may be due to genetic background of this strain.

TABLE 4.4

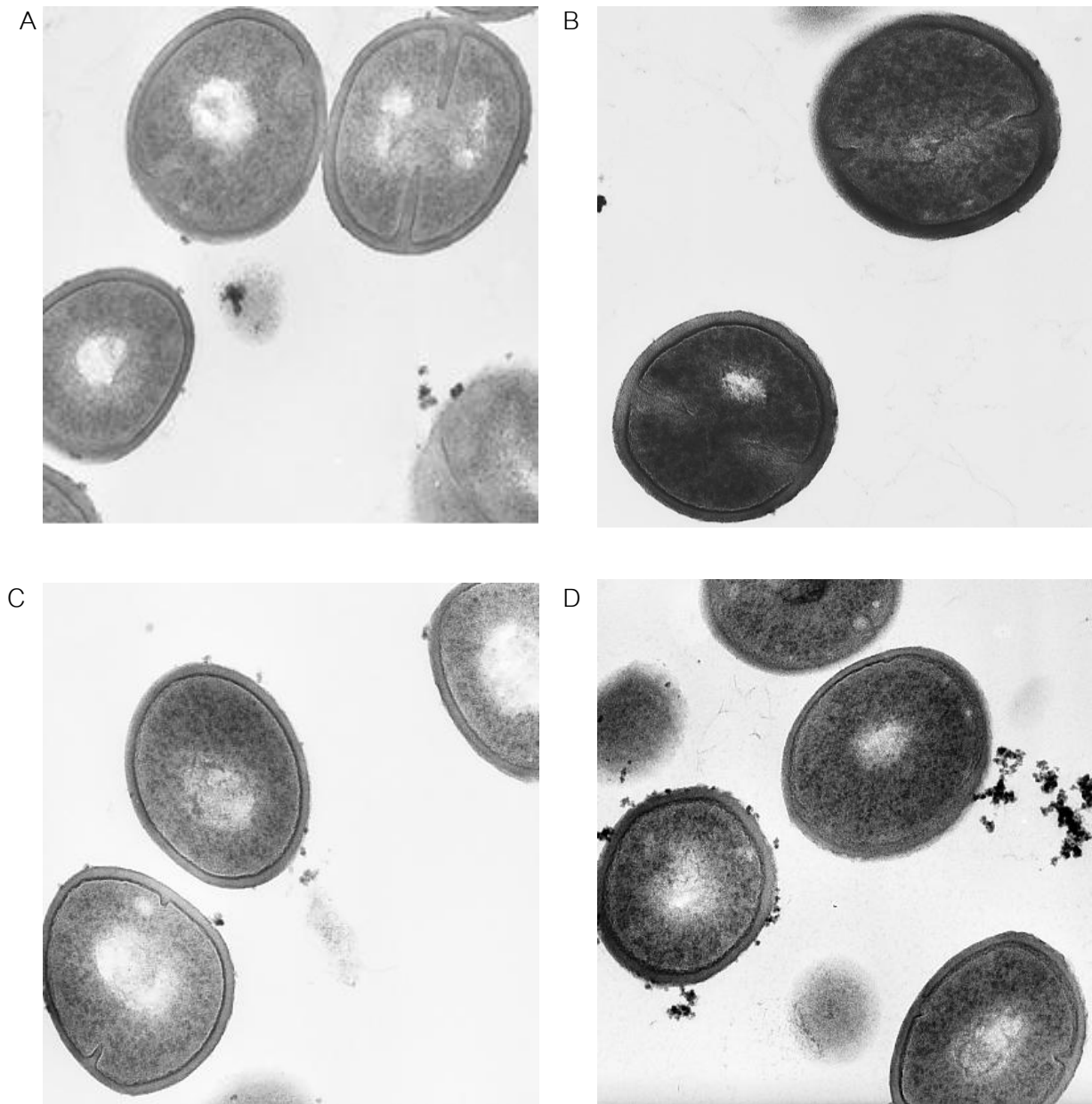
Cell Wall Thickness of VISA Derivatives and Their VSSA Strains

Bacterial Strains	Cell Wall Thickness (nm \pm SD)	
	Bacteria Grown in the Absence of Vancomycin	Bacteria Grown in the Presence of Vancomycin
KY	38.48 \pm 1.31	39.58 \pm 2.40
KY-8-1	52.73 \pm 3.31	53.02 \pm 2.76
SS	45.09 \pm 4.01	46.35 \pm 4.19
SS-8-1	54.64 \pm 2.01	56.16 \pm 2.28
UH7	47.12 \pm 2.57	51.45 \pm 2.08
UH7-8-1	56.21 \pm 3.98	56.41 \pm 4.12
UH9	34.89 \pm 2.62	37.49 \pm 1.72
UH9-8-1	39.54 \pm 1.78	42.64 \pm 3.27

Evaluation of cell wall thickness was performed by measurement from photographs of transmission electron microscope. Four cells of each strain with nearly equatorial cut surfaces were measured. The number of spots, which was measured of each cell, was eight spots.

FIGURE 4.16

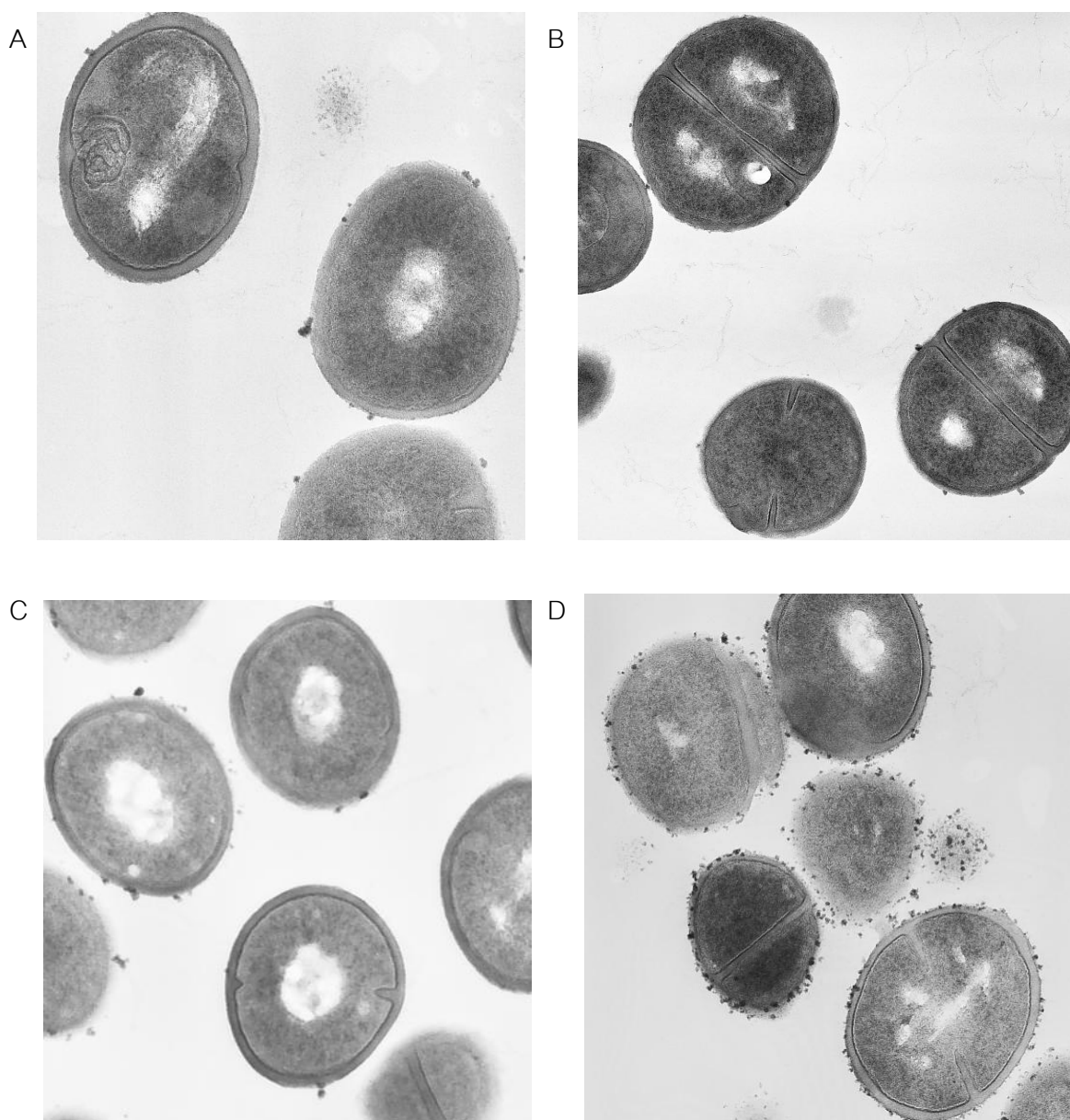
Transmission Electron Micrographs of VISA Derivatives KY-8-1 and Its parental KY



Cell wall morphologies of KY and its VISA derivatives KY-8-1 were examined by transmission electron microscopy. Magnification, x20,000. KY grown in the absence (A) and presence (C) of one-half of the MICs (0.5 µg/ml). KY-8-1 grown in the absence (B) and presence (D) of one-half of the MICs (3.5 µg/ml).

FIGURE 4.17

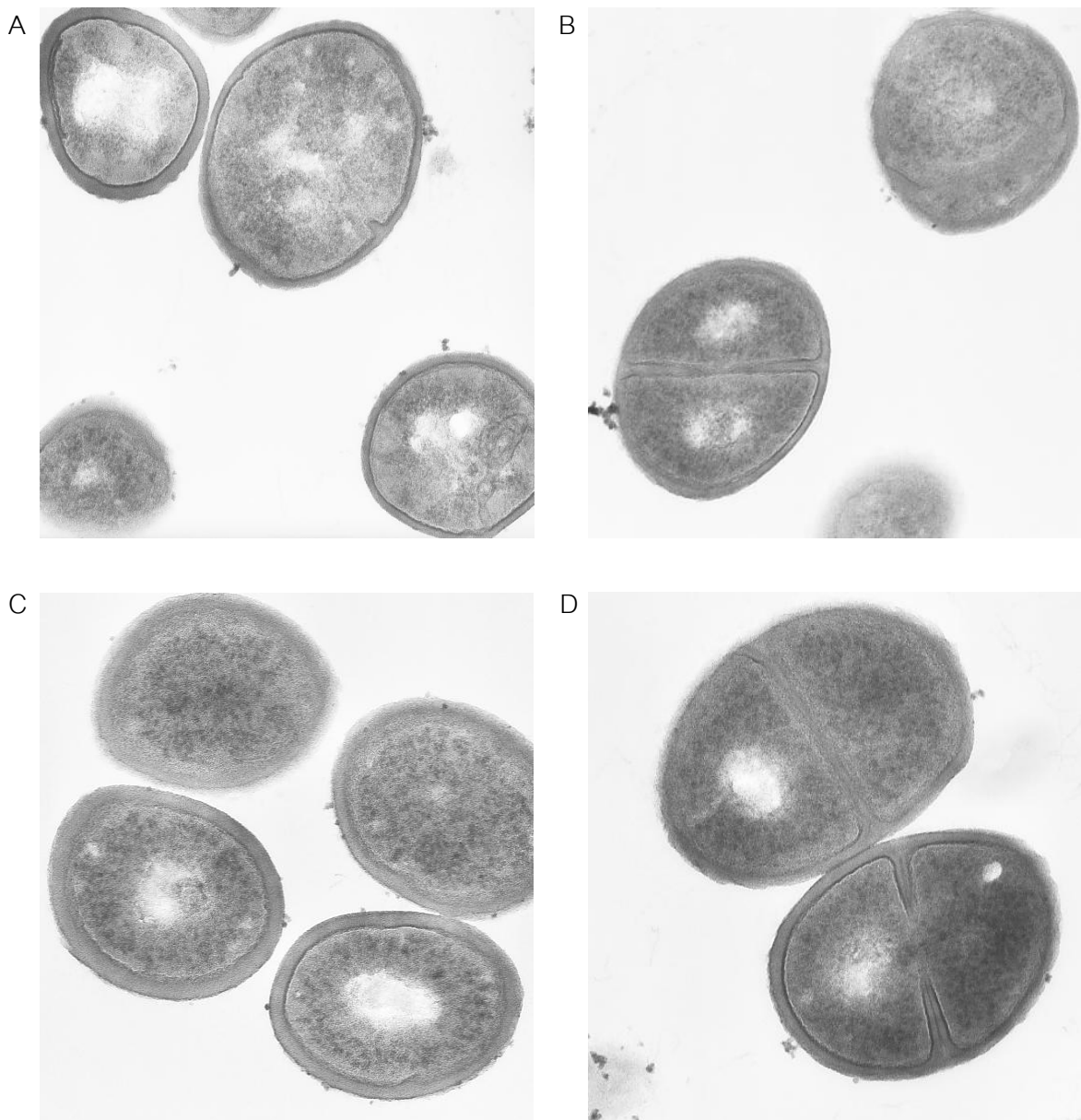
Transmission Electron Micrographs of VISA Derivatives SS-8-1 and Its parental SS



Cell wall morphologies of SS and its VISA derivatives SS-8-1 were examined by transmission electron microscopy. Magnification, x20,000. SS grown in the absence (A) and presence (C) of one-half of the MICs (0.5 µg/ml). SS-8-1 grown in the absence (B) and presence (D) of one-half of the MICs (3.5 µg/ml).

FIGURE 4.18

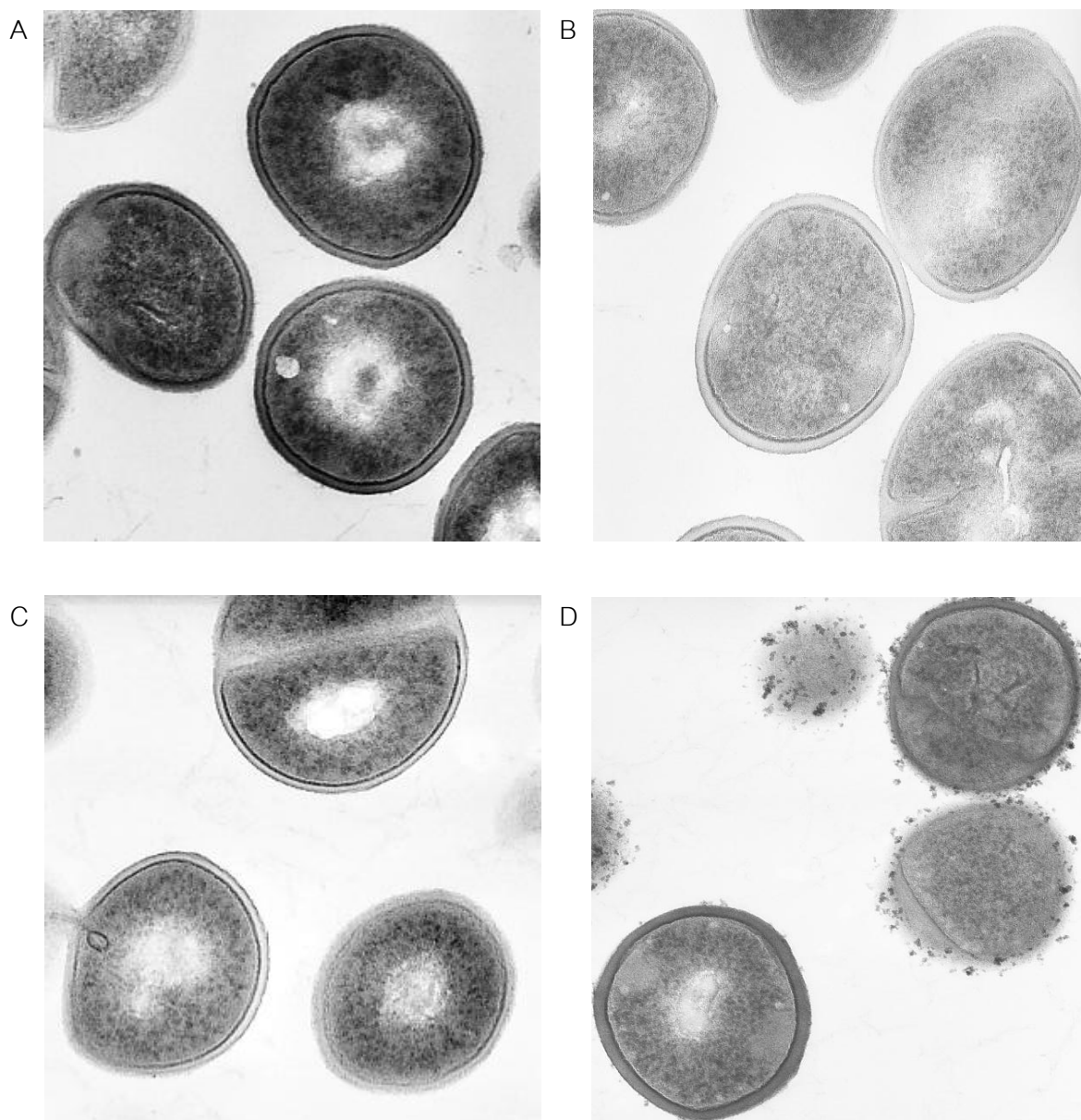
Transmission Electron Micrographs of VISA Derivatives UH7-8-1 and Its parental UH7



Cell wall morphologies of UH7 and its VISA derivatives UH7-8-1 were examined by transmission electron microscopy. Magnification, x20,000. UH7 grown in the absence (A) and presence (C) of one-half of the MICs (0.5 µg/ml). UH7-8-1 grown in the absence (B) and presence (D) of one-half of the MICs (3.5 µg/ml).

FIGURE 4.19

Transmission Electron Micrographs of VISA Derivatives UH9-8-1 and Its parental UH9



Cell wall morphologies of UH9 and its VISA derivatives UH9-8-1 were examined by transmission electron microscopy. Magnification, x20,000. UH9 grown in the absence (A) and presence (C) of one-half of the MICs (0.5 µg/ml). UH9-8-1 grown in the absence (B) and presence (D) of one-half of the MICs (3.5 µg/ml).